Hindawi
International Journal of Antennas and Propagation
Volume 2019, Article ID 8945386, 9 pages
https://doi.org/10.1155/2019/8945386

Research Article

Bandwidth Enhancement and Mutual Coupling Reduction Using a Notch and a Parasitic Structure in a UWB-MIMO Antenna

Jiwan Ghimire,[1] **Kwang-Wook Choi**,[2] **and Dong-You Choi**[1]

[1]*Department of Information and Communication Engineering, Chosun University, 375 Susuk-dong, Dong-gu, Gwangju 501-759, Republic of Korea*
[2]*Department of Electronic and Computer Engineering, Chonnam National University, 77 Yongbong-ro, Yongbong-dong, Buk-gu, Kwangju, Republic of Korea*

Correspondence should be addressed to Dong-You Choi; dychoi@chosun.ac.kr

Received 24 February 2019; Revised 29 April 2019; Accepted 6 May 2019; Published 2 June 2019

Academic Editor: Shiwen Yang

The correlation between the antennas of multiple-input, multiple-output (MIMO) systems in limited spaces and size degrades the performance and capacity by either using complex coupling or decoupling structures. For isolation improvement, this paper presents the simple design of a compact high-isolation ultra-wideband (UWB) MIMO antenna with a circular parasitic element at the back side of the radiating patch, thereby creating the reverse coupling and helping reduce the mutual coupling at the upper part of the frequency bands, and a small rectangular notch at the ground plane to extend the impedance bandwidth of the monopole antenna. This approach eliminates the use of complex coupling or decoupling structures and complex feeding networks. A novel feature of our design is that the MIMO antenna exhibits a very low envelope correlation coefficient (ECC < 0.007) with high diversity gain (DG > 9.99) and wide impedance bandwidth of 139 % from 3.1 to 17.5 GHz applicable for not only UWB application, but also next generation wireless communication, 5G. The high peak gain over the entire UWB and the upper part of the overall frequency band ensure that the antenna can be used in MIMO applications owing to the close agreement between the simulated and measured results.

1. Introduction

The need for high data rates with efficient spectrum management utilizing multiple antennas in a single physical substrate is a recent requirement in modern wireless communication and UWB systems. To that end, multiple-input, multiple-output (MIMO) technology takes advantage of multipath fading problems through diversity gain to improve link reliability, increase data throughput, and improve wireless capacity and range, which is not possible in a single-antenna system [1]. Even though MIMO technology is better than single-input, multiple-output (SIMO) or multiple-input, single-output (MISO) in terms of channel capacity, it has some limitations regarding the correlation between the antennas and realizing space efficiency [2]. Improving the isolation factor or correlation in a MIMO antenna using various types of coupling and decoupling structures is achieved at the expense of size and space [3].

Using decoupling structures such as active devices and passive resonators, implementing defective ground structures (DGSs), electromagnetic bandgap, parasitic elements, adding neutralization lines, shortening pins, and loading slots on the antenna geometry for to avoid mutual coupling and improve the antenna bandwidth are proposed in various studies. In [4], a UWB amplifier was inserted to achieve wideband antenna matching and radiation efficiency. Similarly, a passive microstrip-based feed network was introduced in [5] and a cylindrical dielectric resonator antenna (CDRA) in [6] for good MIMO operations at higher frequencies. A number of radiating elements in MIMO antenna systems were designed to improve isolation with DGS using different shapes (T, F, 4, arch) and slot lines, rectangular rings, and ground slits were also employed [7–14]. In [15], the electromagnetic bandgap structure was applied to closely placed arrays in the ground plane, resulting in a significant reduction of mutual coupling across a wide operating band. The use of parasitic

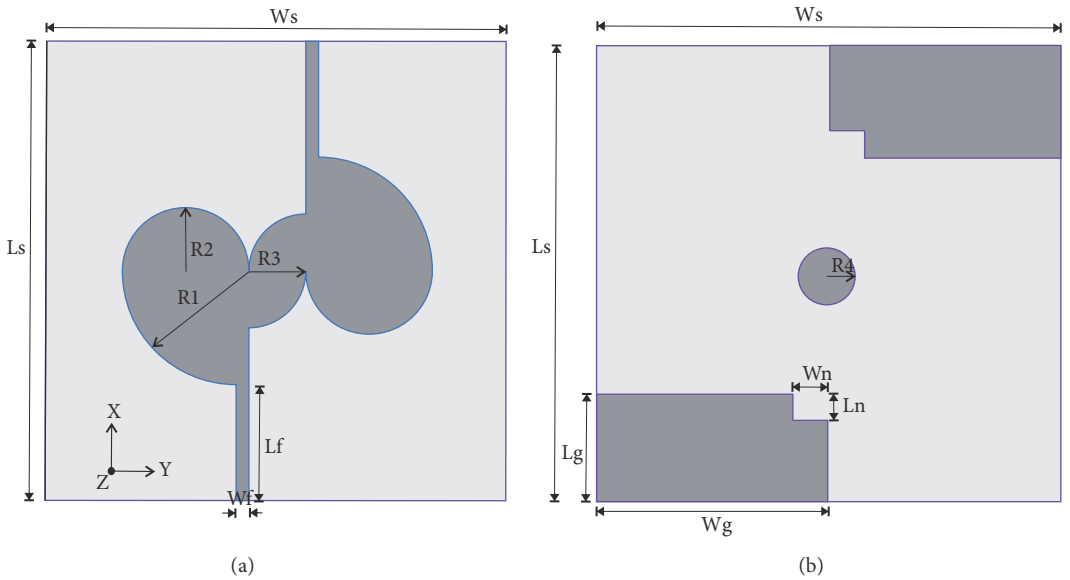

Figure 1: Geometry of the proposed UWB antenna (a) Top view, (b) bottom view of the antenna.

monopoles or resonators helped induce reverse coupling and hence reduced mutual coupling in [16, 17]. In [18], adding a neutralization line increased the effectiveness of the antenna system in terms of isolation and bandwidth within a small space without modifying the ground plane.

Similarly, E, C and H-shaped patch antennas were loaded by U and V slots to achieve desired bandwidth characteristics [24]. In addition, developing efficient bandwidth enhancement with existing different technique in an area of limited size within a MIMO system is still a difficult task.

In this paper, the UWB MIMO antenna with enhanced isolation is proposed. The proposed MIMO antenna has a very low mutual coupling ($|S_{21}/S_{12}| < -21$ dB) and is composed of two monopole antennas with a common radiating surface. The two radiating patches are connected by two quad-circular structures. The ground plane is on the opposite side of the radiating patch etched to increase the impedance bandwidth characteristics. A circular parasitic element introduced at the centre of the substrate acts as an isolator and exhibits low mutual coupling for the upper frequency bands of the antenna. In the absence of coupling or decoupling structures, a good isolation is achieved without the expense of increase in size. The results obtained from the proposed MIMO antenna without the use of complex structures reveal that it has good performance in terms of high impedance bandwidth and antenna gain, high radiation efficiency, high diversity gain, and low envelope correlation coefficient (ECC). The omnidirectional radiation pattern of the purposed MIMO antenna element proves that the antenna possesses good pattern diversity for a MIMO system.

2. Antenna Characteristics

The proposed geometry of the UWB-MIMO antenna is shown in Figure 1, where Figures 1(a) and 1(b) represent the top and bottom geometrical view of the substrate with

Table 1: Dimensions of the Antenna Parameters.

Parameter	Dimension (mm)
Ls	65
Ws	65
Lf	16.3
R1	17.8
R2	8.9
R3	8
R4	4
Lg	16
Wg	32.7
Ln	4
Wn	5
Wf	1.8

the optimal dimension listed in Table 1. The antenna was designed on a Taconic substrate ($\varepsilon_r = 4.5$, $\tan\delta = 0.0035$). The size of the antenna is 65 mm × 65 mm × 1.62 mm. The antenna is composed of a microstrip patch with a common radiating patch and a ground plane designed on the top and bottom side of the substrate respectively. Here, to meet the operating frequency requirement, the return loss at the 10 dB lower frequency bandwidth is adjusted to 3.1 GHz approximated using the following frequency calculation [25].

$$f_n = \frac{c}{2l_t\sqrt{1+\varepsilon_r/2}}, \quad (1)$$

where f_n is the first operating frequency, c is the speed of light in the vacuum, and l_t is the combine total effective lengths of the circular patch radii R1 and R2. The feed line and a small notch in the ground plane, employed to obtain the line characteristic impedance of 50 Ω, are set to 1.8 mm and 4 mm × 5 mm, respectively. The radiating patch is structurally

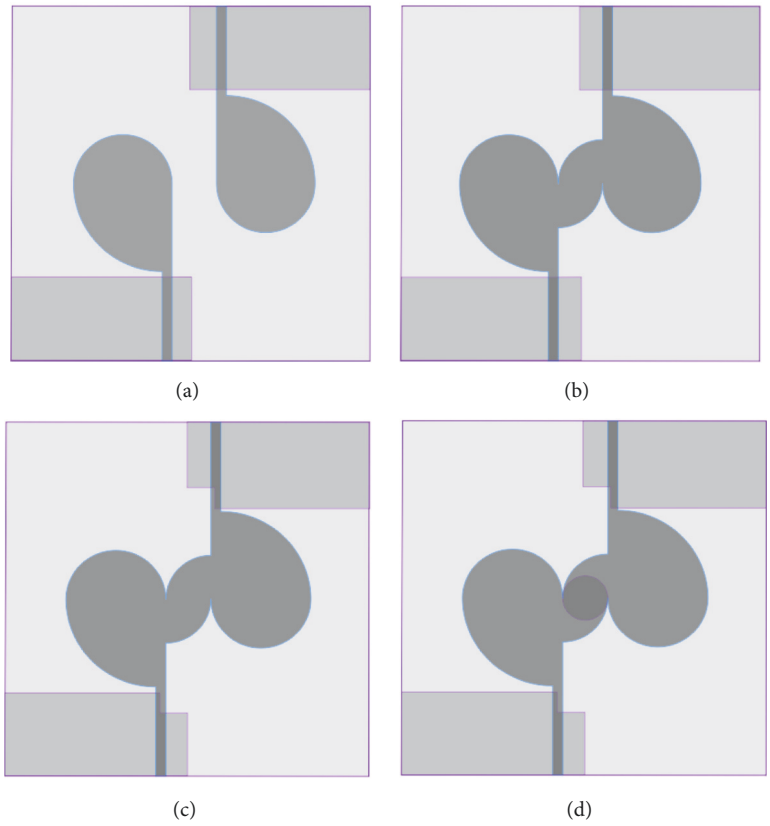

Figure 2: Geometry of the proposed UWB antenna with different evolution steps. (a) Without the connecting radiation patch, (b) with the connecting radiation patch, (c) with the ground plane etched, and (d) with the parasitic resonator.

a combination of a quad circular structure with a semi-circle of half the radius of the quad circle placed on its top. The two radiating patches are commonly connected by two small quad circular structures positioned opposite to each other, where the circular parasitic strip is located below it along the centre of the substrate to improve isolation between the monopole antennas. The need of connecting two radiating patches by two small quad circles is to not only improve the isolation but also have a common signal reference weather it is a ground plane or the radiating patch. A split in both ground plane and radiating patch is not practical, since in the real system; the signal should have the common reference plane so that all signal levels within the systems can be interpreted properly based on that reference level [17]. However, the proposed design is similar to a microstrip patch antenna with feeding points placed opposite to each other; the optimized antenna structure, isolation enhancement without the use of coupling and decoupling structure, makes it preferable in terms of bandwidth, diversity gain, and multiplexing efficiency, which are the significant parameters for any diversity antennas.

3. Design Strategy

Figure 2 illustrates the antenna designing steps and the effect of each step on the antenna bandwidth and mutual coupling are shown in Figure 3. Figure 2(a) shows that the antenna design with radiating patches facing indirectly opposite to each other allows space utilization within a limited space of the antenna. Similarly, the geometrical structure of the radiating patch enables the MIMO antenna to be directional, which could supply good pattern diversity for the MIMO system. The simulated parameters of the antenna reflection coefficient (S_{11}) and coupling coefficient (S_{21}) in Figures 3(a) and 3(b) reveal that the antenna has poor isolation in the higher frequency range and a high impedance mismatch in the entire UWB range for the antenna shown in Figure 2(a). With the placement of two quad circular structures connecting two radiating patches (Figure 2(b)), mutual coupling between the proposed antennas is reduced, but the characteristic line impedance of the antenna remains the same as that of the antenna design taken at the first stage. Further, to improve the impedance bandwidth of the antenna in the entire UWB range, a small rectangular etching is carved at the ground plane (Figure 2(c)). The etching not only improves the characteristic line impedance but also decreases the isolation factors in the lower frequency spectrum of the proposed UWB MIMO antenna with a slight increase in isolation factor at the upper-frequency range. A circular parasitic microstrip patch resonator is introduced at the backside of the substrate plane (Figure 2(d)). The current flowing in the radiating patch excites the resonator. The excited reverse current on the resonator prevents the flow of current in the other radiating patch, preventing it from further coupling; on properly designing the antenna

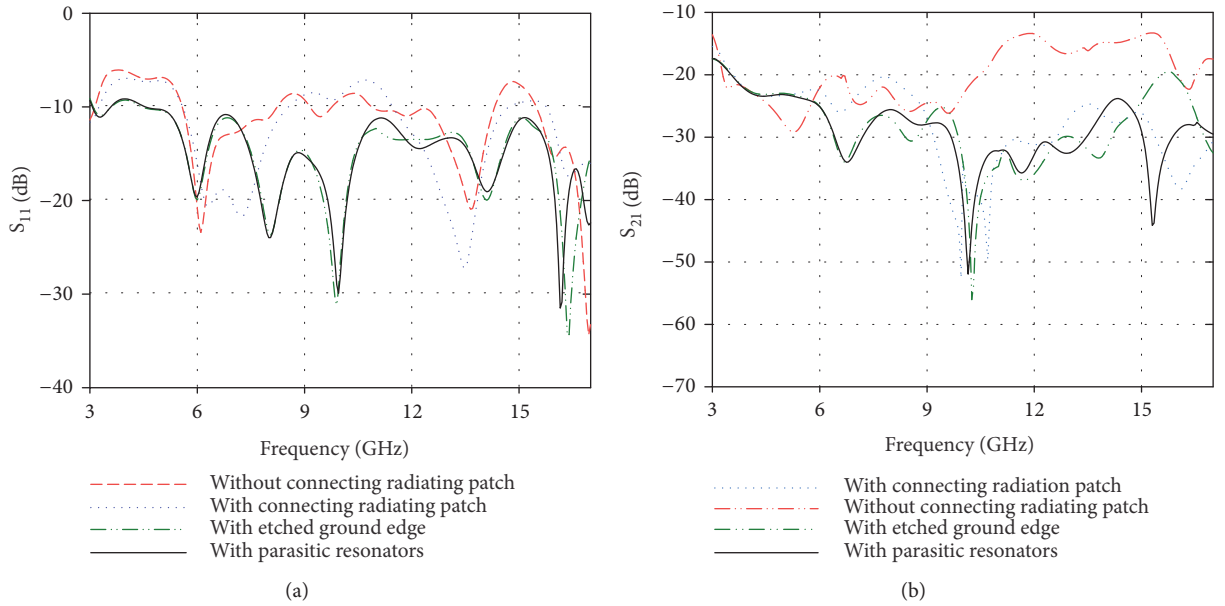

FIGURE 3: Simulated S-parameters to illustrate different stages of antenna variation in design for improving the antenna bandwidth and reducing the mutual coupling (a) Simulated reflection coefficient S_{11} (dB), (b) simulated coupling coefficient S_{21} (dB).

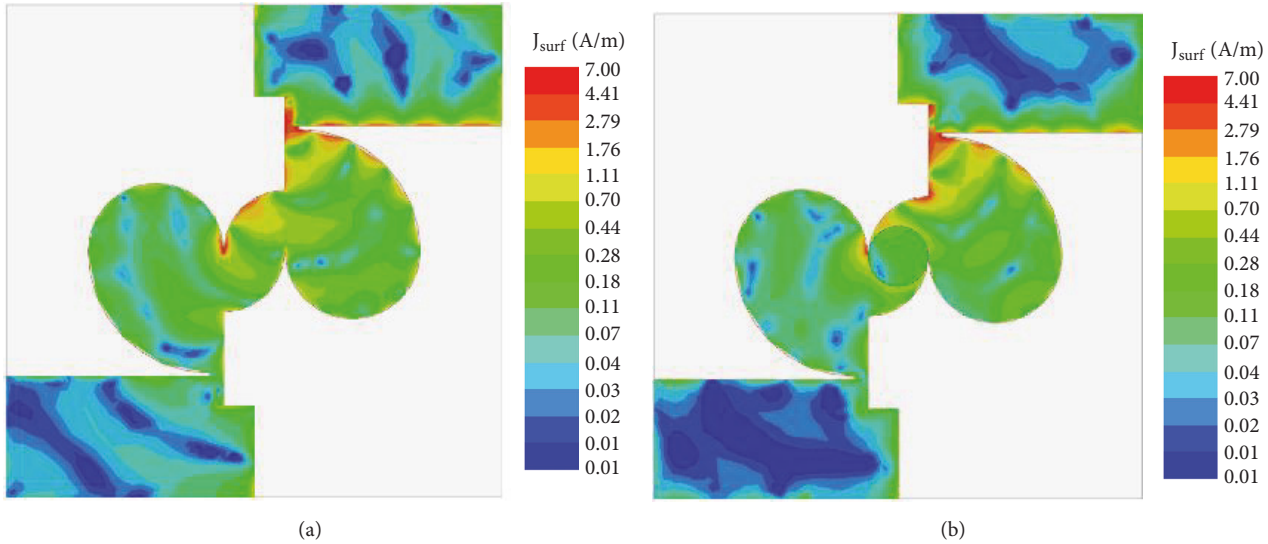

FIGURE 4: Simulated surface current distribution at 16.5 GHz: (a) Without circular parasitic resonator, (b) with the resonator.

configuration, the mutual coupling between the radiating patch gets reduced considerably.

The surface current distribution along the radiating and ground patch validates the antenna performance of reducing the mutual coupling. As a comparison, the current distributions with and without the circular parasitic monopoles are plotted in Figure 4, when one of the ports is excited. As shown in Figure 4(a), high coupling is achieved at the other radiating patch and the ground plane because the current concentration is equally spread all around the patch and the ground plane significantly. By the insertion of the circular resonating structure depicted in Figure 4(b), it can be observed that the current is concentrated at the radiating patch of the excited port and gets trapped all around the periphery of the circular resonating structure. Because of this effect, the ground plane of the other radiator and the patch has coupled much less current concentration, and hence less isolation is achieved in between the two radiating patches. In addition, the simulation result shows that most of the current above 14.7 GHz is concentrated around the resonating patch, which explains the reduced mutual coupling (S_{21}) observed in Figure 3(b).

4. Result and Discussion

For the optimization and simulation of the proposed antenna, the commercially available High-Frequency Structure

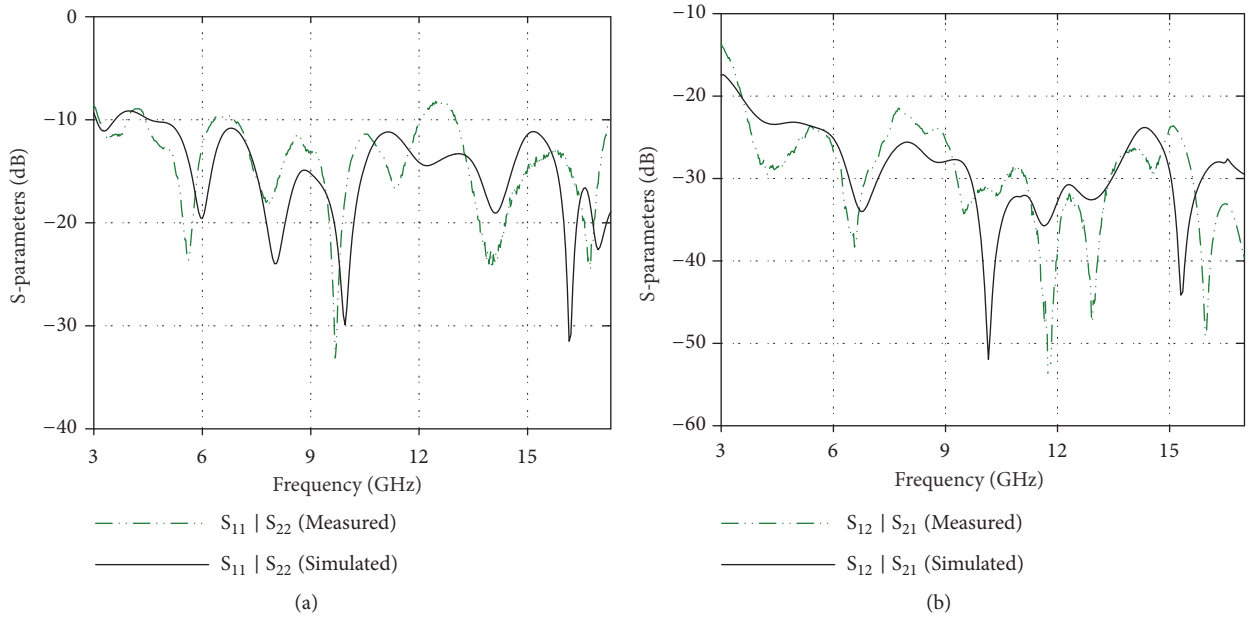

Figure 5: Simulated and measured S-parameters of the proposed UWB-MIMO antenna: (a) S_{11} (dB), (b) S_{21} (dB).

Simulator (HFSS) software is used. The simulation and measurement results are shown in Figure 5; Figure 5(a) shows impedance bandwidth with $S_{11} < -10$ dB from 3.1 to 17.5 GHz. The mutual coupling between the antennas (S_{21}) shown in Figure 5(b) is below −15 dB for 3.1–3.5 GHz and below −21 dB over 3.5–17.5 GHz with close agreement between the measured and simulated results. The simulated and measured reflection coefficients differ slightly and can be indorsed by the losses taking place in connector, imperfect soldering and fabrication errors.

The measured and simulated 2D radiation patterns at 4.5, 6.5, 11.5, and 16.5 GHz frequency are shown in Figures 6(a), 6(b), 6(c), and 6(d), respectively. The measurements were taken with one of the ports terminated by a 50-Ω load and vice versa. The radiation patterns are almost omnidirectional in both the E-plane (x–z plane) and H-plane (y–z plane), which is one of the required characteristics for a MIMO antenna.

In order to verify the capability of the proposed MIMO antenna, ECC between the antennas must be as low as possible; a lower ECC signifies higher pattern diversity. The ECC between the two antenna elements can be calculated by [26]

$$ECC = \frac{\left|S_{11}^{*}S_{12} + S_{21}^{*}S_{22}\right|^{2}}{\left(1 - \left|S_{11}\right|^{2} - \left|S_{21}\right|^{2}\right)\left(1 - \left|S_{22}\right|^{2} - \left|S_{12}\right|^{2}\right)} \quad (2)$$

From the measurement results of return loss and isolation factor, the ECC was analysed as shown in Figure 8. The ECC ideally should be zero; practically, < 0.5 is an acceptable limit.

Conventionally, the overall effect of a MIMO antenna is characterized by diversity gain (DG) and MIMO capacity. However, MIMO capacity is the complicated function of the antenna parameters. To simplify the antenna design, a simple and intuitive metric like multiplexing efficiency and TARC are proposed. The multiplexing efficiency defines the losses or degradation of power efficiency required when using a MIMO antenna under test to achieve the same performance or capacity as that of a reference antenna system in the same propagation channel within uniform 3D angular power spectrum. The signal-to-noise ratio (SNR) degradation due to MIMO antenna –channel losses for a given MIMO capacity, η_{mux} is given by [27]

$$\eta_{mux} = \sqrt{\left(1 - \left|\rho_c{}^{2}\right|\right)\eta_1\eta_2} \quad (3)$$

where $\eta_1\eta_2$ are the total efficiency of two radiating antenna elements and ρ_c represents the complex correlation coefficient between them. Since the total efficiency of the antenna is very high, for this ECC is nearly equal to $|\rho_c{}^{2}|$.The DG of the proposed UWB MIMO antenna can be calculated using relation

$$DG = 10\sqrt{1 - ECC^{2}} \quad (4)$$

All the ECC values are less than 0.007, and the DG is high, greater than 9.99 for the entire frequency band. The realized gain and the multiplexing efficiency are shown in Figure 9 where its high measurement values on the entire frequency range make the antenna applicable for UWB, 5G communication devices, and sensor applications. The fabricated prototype of UWB MIMO antenna with top and bottom view is shown in Figures 7(a) and 7(b).

Figure 10 shows the plot of the total active reflection coefficient (TARC) where the value of TARC of the proposed antenna is less than -1.3 dB for the entire frequency band. TARC calculates the actual antenna behaviour in terms of ratio of square root of the sum of powers of reflected wave to the incident wave. By predicting the return loss of the overall

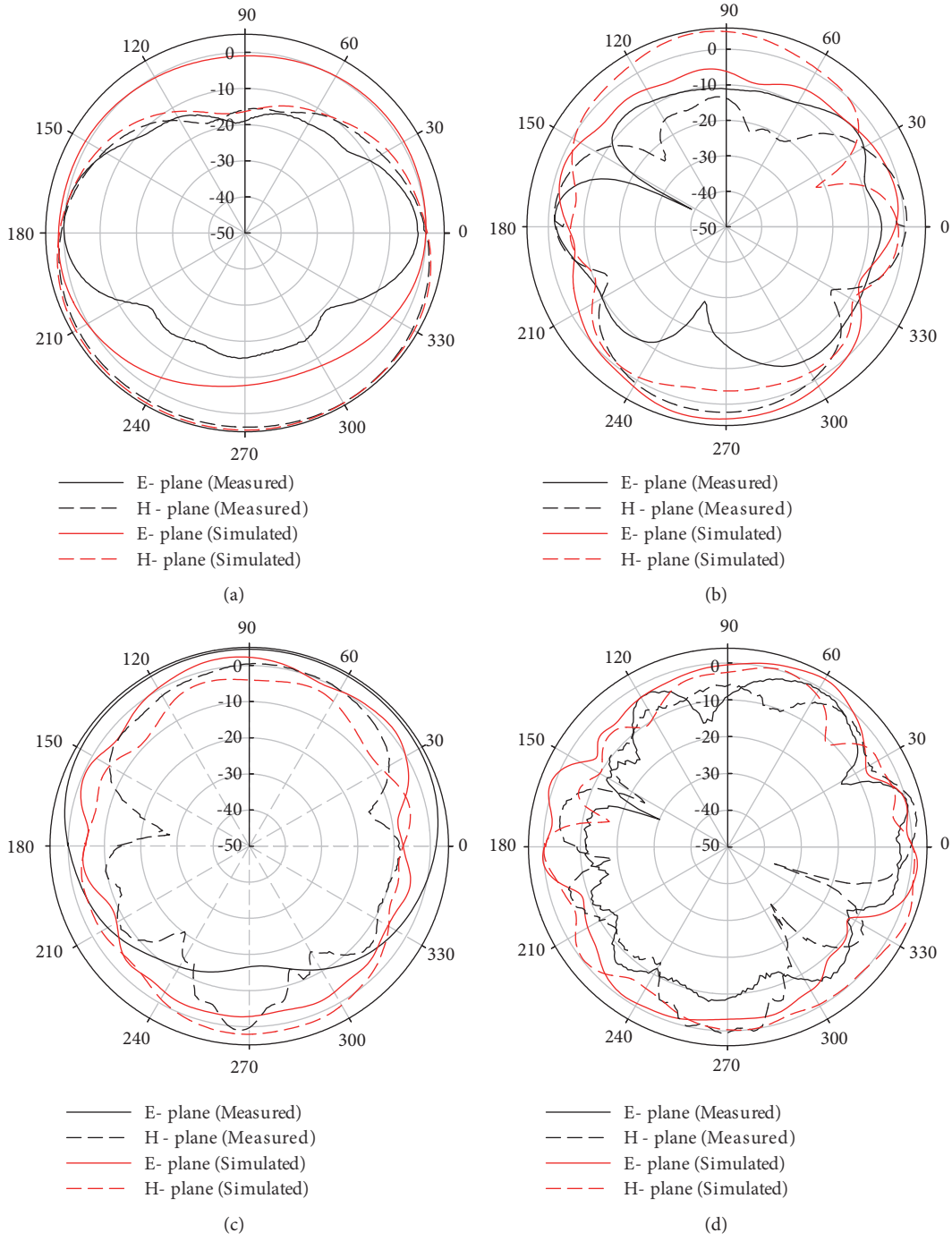

Figure 6: Measured and simulation radiation pattern at (a) 4.5, (b) 6.5, (c) 11.5, and (d) 16.5 GHz.

2X2 MIMO antenna system TARC can be calculated by the following relations [28].

$$\text{TARC} = \sqrt{\frac{(S_{11} + S_{12})^2 + (S_{21} + S_{22})^2}{2}} \quad (5)$$

The comparison of the proposed MIMO Antenna between other existing antennas in the literature is listed in Table 2. The designed antenna has a wide impedance bandwidth overall, with good isolation factor and diversity gain proving that the antenna is a good candidate for MIMO application.

5. Conclusion

The design of a compact, high-isolation ultra-wideband (UWB) MIMO antenna with a circular parasitic element at the backside of the radiating patch is proposed. Without the presence of coupling or decoupling element and by

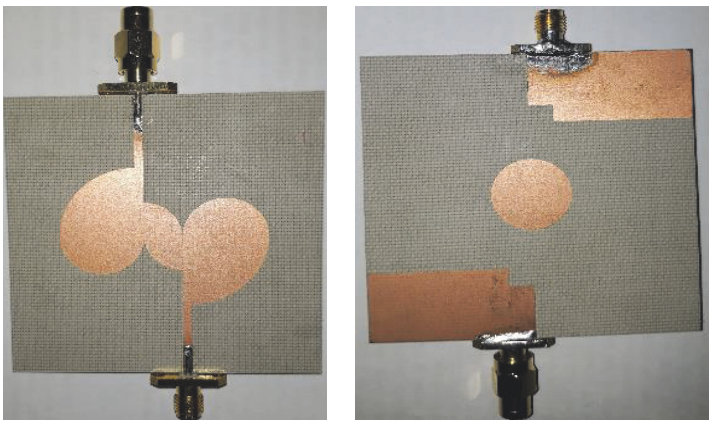

(a) (b)

Figure 7: Fabricated UWB MIMO Antenna: (a) Top view, (b) bottom view.

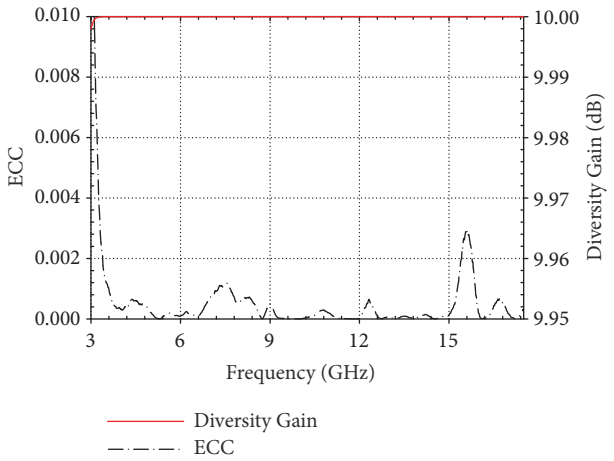

Figure 8: Measured ECC and DG of the proposed antenna.

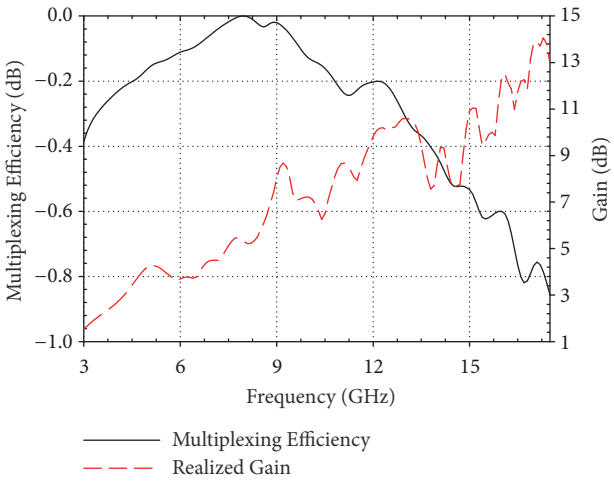

Figure 9: Realized gain and multiplexing efficiency of the proposed antenna.

Table 2: Performance Comparison of Existing Antennas.

Ref.	Size (mm)	Bandwidth (GHz)	Isolation (dB)	ECC	Diversity Gain
[12]	30 × 50	2.5–14.5	< −20	< 0.04	> 7.4
[19]	60 × 40	3.1–10.6	< −20	< 0.06	> 9.89
[20]	50 × 80	3.1–10.6	< −17	<0.056	NA
[21]	32 × 32	3.1–10.6	< −15	< 0.04	NA
[22]	26 × 40	2.1–10.6	< −15	NA	NA
[23]	45 × 25	3 –12	< −15	<0.2	> 9.79
Proposed Work	65 × 65	3.1–17.5	< −20	< 0.007	> 9.99

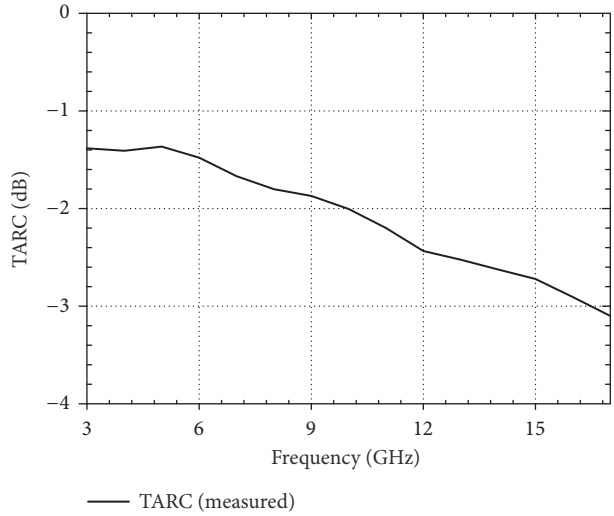

Figure 10: TARC for the proposed MIMO antenna.

introducing a parasitic circular structure, high isolation is achieved at the upper part of the frequency band, whereas a small rectangular notch at the ground plane helps widen the antenna operating bandwidth and improve the impedance matching of the two connecting radiating elements. To validate the design strategy for reducing mutual coupling and increase the operating bandwidth, essential features such as ECC (< 0.007), DG (> 9.99), isolation less than -21dB, almost omnidirectional radiation pattern and high gain performance and multiplexing efficiency were shown and verified with simulation and measurement results to describe the MIMO performance of the UWB antenna.

Data Availability

The data used to support the findings of this study are included within the article.

Conflicts of Interest

The authors declare that they have no competing interests.

Acknowledgments

This research was supported by the Basic Science Research Program through the National Research Foundation of Korea (NRF) funded by the Ministry of Education (2016R1D1A1B03931806). Also, the research was partially funded by the MIST (Ministry of Science & ICT), Korea, under the National Program for Excellence in SW supervised by the IITP (Institute for Information & communications Technology Promotion) (2017-0-00137).

References

[1] M. A. Jensen and J. W. Wallace, "A review of antennas and propagation for MIMO wireless communications," *IEEE Transactions on Antennas and Propagation*, vol. 52, no. 11, pp. 2810–2824, 2004.

[2] J. Park and B. Clerckx, "Multi-User linear precoding for multi-polarized massive MIMO system under imperfect CSIT," *IEEE Transactions on Wireless Communications*, vol. 14, no. 5, pp. 2532–2547, 2015.

[3] I. Nadeem and D.-Y. Choi, "Study on mutual coupling reduction technique for mimo antennas," *IEEE Access*, vol. 7, pp. 563–586, 2019.

[4] S. K. Dhar, M. S. Sharawi, O. Hammi, and F. M. Ghannouchi, "An active integrated ultra-wideband MIMO antenna," *Institute of Electrical and Electronics Engineers. Transactions on Antennas and Propagation*, vol. 64, no. 4, pp. 1573–1578, 2016.

[5] M. T. Hussain, M. S. Sharawi, S. Podilchack, and Y. M. M. Antar, "Closely packed millimeter-wave MIMO antenna arrays with dielectric resonator elements," in *Proceedings of the 10th*

European Conference on Antennas and Propagation, EuCAP 2016, pp. 1–4, Switzerland, April 2016.

[6] A. Sharma, G. Das, and R. K. Gangwar, "Design and analysis of tri-band dual-port dielectric resonator based hybrid antenna for WLAN/WiMAX applications," *IET Microwaves, Antennas & Propagation*, vol. 12, no. 6, pp. 986–992, 2018.

[7] M. S. Sharawi, A. B. Numan, M. U. Khan, and D. N. Aloi, "A dual-element dual-band MIMO antenna system with enhanced isolation for mobile terminals," *IEEE Antennas and Wireless Propagation Letters*, vol. 11, pp. 1006–1009, 2012.

[8] M. A. Abdalla and A. A. Ibrahim, "Compact and closely spaced metamaterial MIMO antenna with high isolation for wireless applications," *IEEE Antennas and Wireless Propagation Letters*, vol. 12, pp. 1452–1455, 2013.

[9] Y. Wu and Q. Chu, "Dual-band multiple input multiple output antenna with slitted ground," *IET Microwaves, Antennas & Propagation*, vol. 8, no. 13, pp. 1007–1013, 2014.

[10] C.-M. Luo, J.-S. Hong, and L.-L. Zhong, "Isolation Enhancement of a Very Compact UWB-MIMO Slot Antenna with Two Defected Ground Structures," *IEEE Antennas and Wireless Propagation Letters*, vol. 14, pp. 1766–1769, 2015.

[11] S. F. Jilani and A. Alomainy, "Millimetre-wave T-shaped MIMO antenna with defected ground structures for 5G cellular networks," *IET Microwaves, Antennas & Propagation*, vol. 12, no. 5, pp. 672–677, 2018.

[12] A. Iqbal, O. A. Saraereh, A. W. Ahmad, and S. Bashir, "Mutual Coupling Reduction Using F-Shaped Stubs in UWB-MIMO Antenna," *IEEE Access*, 2017.

[13] R. Karimian, H. Oraizi, S. Fakhte, and M. Farahani, "Novel F-shaped quad-band printed slot antenna for WLAN and WiMAX MIMO systems," *IEEE Antennas and Wireless Propagation Letters*, vol. 12, pp. 405–408, 2013.

[14] B. Yang, M. Chen, and L. Li, "Design of a four-element WLAN/LTE/UWB MIMO antenna using half-slot structure," *AEÜ - International Journal of Electronics and Communications*, vol. 93, pp. 354–359, 2018.

[15] Q. Li, A. P. Feresidis, M. Mavridou, and P. S. Hall, "Miniaturized double-layer EBG structures for broadband mutual coupling reduction between UWB monopoles," *IEEE Transactions on Antennas and Propagation*, vol. 63, no. 3, pp. 1168–1171, 2015.

[16] Z. Li, Z. Du, M. Takahashi, K. Saito, and K. Ito, "Reducing mutual coupling of MIMO antennas with parasitic elements for mobile terminals," *IEEE Transactions on Antennas and Propagation*, vol. 60, no. 2, pp. 473–481, 2012.

[17] S. Zhang and G. F. Pedersen, "Mutual Coupling Reduction for UWB MIMO Antennas with a Wideband Neutralization Line," *IEEE Antennas and Wireless Propagation Letters*, vol. 15, pp. 166–169, 2016.

[18] M. S. Sharawi, "Current misuses and future prospects for printed multiple-input, multiple-output antenna systems [wireless corner]," *IEEE Antennas and Propagation Magazine*, vol. 59, no. 2, pp. 162–170, 2017.

[19] C.-X. Mao, Q.-X. Chu, Y.-T. Wu, and Y.-H. Qian, "Design and investigation of closely-packed diversity UWB slot-antenna with high isolation," *Progress in Electromagnetics Research C*, vol. 41, pp. 13–25, 2013.

[20] S. S. Jehangir and M. S. Sharawi, "A miniaturized uwb biplanar yagi-like mimo antenna system," *IEEE Antennas and Wireless Propagation Letters*, vol. 16, pp. 2320–2323, 2017.

[21] J. Ren, W. Hu, Y. Yin, and R. Fan, "Compact printed MIMO antenna for UWB applications," *IEEE Antennas and Wireless Propagation Letters*, vol. 13, pp. 1517–1520, 2014.

[22] L. Liu, S. W. Cheung, and T. I. Yuk, "Compact MIMO antenna for portable devices in UWB applications," *IEEE Transactions on Antennas and Propagation*, vol. 61, no. 8, pp. 4257–4264, 2013.

[23] R. Mathur and S. Dwari, "Compact CPW-Fed ultrawideband MIMO antenna using hexagonal ring monopole antenna elements," *AEÜ - International Journal of Electronics and Communications*, vol. 93, pp. 1–6, 2018.

[24] Y. Chen, S. Yang, and Z. Nie, "Bandwidth enhancement method for low profile E-shaped microstrip patch antennas," *IEEE Transactions on Antennas and Propagation*, vol. 58, no. 7, pp. 2442–2447, 2010.

[25] A. B. Constantine, "Antenna theory: analysis and design," in *Microstrip Antennas*, pp. 64-65, John Wiley & Sons, 3rd edition, 2005.

[26] S. Blanch, J. Romeu, and I. Corbella, "Exact representation of antenna system diversity performance from input parameter description," *IEEE Electronics Letters*, vol. 39, no. 9, pp. 705–707, 2003.

[27] R. Tian, B. K. Lau, and Z. Ying, "Multiplexing efficiency of MIMO antennas in arbitrary propagation scenarios," in *Proceedings of the 6th European Conference on Antennas and Propagation (EuCAP '12)*, pp. 373–377, IEEE, Prague, Czech Republic, March 2012.

[28] M. Manteghi and Y. Rahmat-Samii, "Multiport characteristics of a wide-band cavity backed annular patch antenna for multipolarization operations," *IEEE Transactions on Antennas and Propagation*, vol. 53, no. 1, pp. 466–474, 2005.